Science of the Total Environment 573 (2016) 27–38

Contents lists available at ScienceDirect

Science of the Total Environment

journal homepage: www.elsevier.com/locate/scitotenv

Spatial variation in diesel-related elemental and organic $PM_{2.5}$ components during workweek hours across a downtown core

Brett J. Tunno *, Jessie L.C. Shmool, Drew R. Michanowicz, Sheila Tripathy, Lauren G. Chubb, Ellen Kinnee, Leah Cambal, Courtney Roper, Jane E. Clougherty

University of Pittsburgh Graduate School of Public Health, Department of Environmental and Occupational Health, Pittsburgh, PA, United States

HIGHLIGHTS

- Sampling sites were allocated according to vehicular, truck, and bus traffic.
- Highest sampling density (nearly 13 monitors/km^2) study to our knowledge.
- Greater concentration differences observed across sites than between seasons.
- LUR models suggested a strong influence of bus-related emissions.
- We found substantial variation in diesel-related concentrations in a small urban area.

GRAPHICAL ABSTRACT

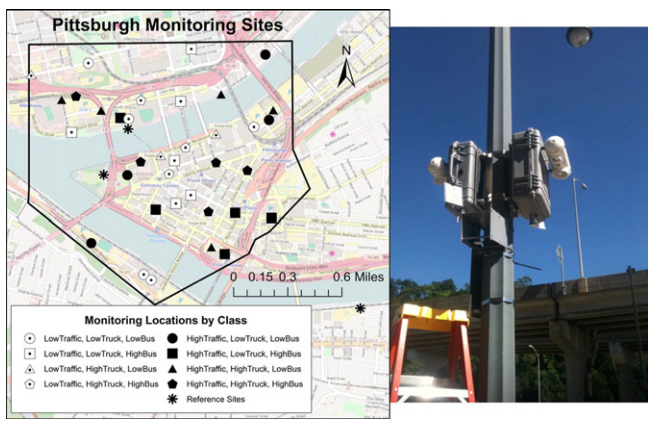

ARTICLE INFO

Article history:
Received 19 May 2016
Received in revised form 2 August 2016
Accepted 3 August 2016
Available online 19 August 2016

Editor: D. Barcelo

Keywords:
Air pollution monitoring
Black carbon (BC)
Elemental constituents
Fine particulate matter ($PM_{2.5}$)
Geographic information systems (GIS)
Land use regression (LUR)
Organic compounds

ABSTRACT

Capturing intra-urban variation in diesel-related pollution exposures remains a challenge, given its complex chemical mix, and relatively few well-characterized ambient-air tracers for the multiple diesel sources in densely-populated urban areas. To capture fine-scale spatial resolution (50 × 50 m grid cells) in diesel-related pollution, we used geographic information systems (GIS) to systematically allocate 36 sampling sites across downtown Pittsburgh, PA, USA (2.8 km^2), cross-stratifying to disentangle source impacts (i.e., truck density, bus route frequency, total traffic density). For buses, outbound and inbound trips per week were summed by route and a kernel density was calculated across sites. Programmable monitors collected fine particulate matter ($PM_{2.5}$) samples specific to workweek hours (Monday–Friday, 7 am–7 pm), summer and winter 2013. Integrated filters were analyzed for black carbon (BC), elemental carbon (EC), organic carbon (OC), elemental constituents, and diesel-related organic compounds [i.e., polycyclic aromatic hydrocarbons (PAHs), hopanes, steranes]. To our knowledge, no studies have collected this suite of pollutants with such high sampling density, with the ability to capture spatial patterns during specific hours of interest. We hypothesized that we would find substantial spatial variation for each pollutant and significant associations with key sources (e.g. diesel and gasoline vehicles), with higher concentrations near the center of this small downtown core. Using a forward stepwise approach, we developed seasonal land use regression (LUR) models for $PM_{2.5}$, BC, total EC, OC, PAHs, hopanes, steranes, aluminum (Al), calcium (Ca), and iron (Fe). Within this small domain, greater concentration differences were observed in most pollutants across sites, on average, than between seasons. Higher $PM_{2.5}$ and BC concentrations were

* Corresponding author at: Department of Environmental and Occupational Health, University of Pittsburgh Graduate School of Public Health, Bridgeside Point, 100 Technology Drive, Room 529, Pittsburgh, PA 15219-3130, United States.
E-mail address: Bjt25@pitt.edu (B.J. Tunno).

http://dx.doi.org/10.1016/j.scitotenv.2016.08.011
0048-9697/© 2016 The Authors. Published by Elsevier B.V. This is an open access article under the CC BY-NC-ND license (http://creativecommons.org/licenses/by-nc-nd/4.0/).

found in the downtown core compared to the boundaries. PAHs, hopanes, and steranes displayed different spatial patterning across the study area by constituent. Most LUR models suggested a strong influence of bus-related emissions on pollution gradients. Buses were more dominant predictors compared to truck and vehicular traffic for several pollutants. Overall, we found substantial variation in diesel-related concentrations in a very small downtown area, which varied across elemental and organic components.

© 2016 The Authors. Published by Elsevier B.V. This is an open access article under the CC BY-NC-ND license (http://creativecommons.org/licenses/by-nc-nd/4.0/).

1. Introduction

Diesel particulate matter (DPM) is a complex mixture of solid particles (e.g., organic compounds and elemental carbon) and liquid particles suspended in gas, typically formed from unburned fuel and/or lubricating oil (Eastwood, 2008). DPM has been identified as a toxic air contaminant and probable human carcinogen by the EPA, capable of causing premature death, and cardiovascular and respiratory health problems (Sydbom et al., 2001; Hesterberg et al., 2012; Kagawa, 2002; Ristovski et al., 2012). Given generally higher diesel-related exposures in dense urban areas, DPM has tremendous importance for public health. To date, however, sampling technologies and analytic techniques have not been able to precisely measure DPM within fine particulate matter ($PM_{2.5}$), nor to examine spatial variation in DPM exposures across urban cores during key hours of interest for human exposures (e.g., during workweek hours, rush hours) (CDC, 2003). To our knowledge, no air pollution studies have assessed a wide variety of organic and elemental constituents using time-integrated samplers across a very high sample density. This approach could enrich our understanding of spatial patterning in exposures to diesel-related pollutants.

Because a large portion of DPM is carbon, elemental carbon (EC) or black carbon (BC, reflectance) have been commonly used as surrogates (Noll et al., 2007; Cyrys et al., 2003; Keuken et al., 2012). These components and most others in DPM, however, are not specific to DPM (CDC, 2003). For example, polycyclic aromatic hydrocarbons (PAHs) also arise from other transportation and industrial processes with incomplete combustion (Noth et al., 2011). Hopanes and steranes are present in crude oil and are used as motor vehicle exhaust markers (Jedynska et al., 2014). As such, there is a need for more clearly identifying effective tracers, or tracer suites, associated with diesel emissions in urban areas.

Spatial saturation campaigns across urban areas have been used to identify key modifiable pollution sources, and to improve air pollution exposure estimates for epidemiology (Shmool et al., 2014; Tunno et al., 2015a; Clougherty et al., 2008; Ross et al., 2006; Matte et al., 2013; Briggs et al., 2000; Basagana et al., 2013). However, relatively few have focused on organic compounds (Larson et al., 2007; Schulte et al., 2015). While it is important to characterize full intra-urban gradients, the saturation design is also well-suited to target specific areas with complex source mixes. Because these campaigns often cover relatively large (i.e., ~350 to 2000 km^2) and diverse (i.e., urban-suburban) areas, they may lack the specificity to quantify exposure differences across smaller areas, or to characterize locally-important emissions sources (e.g., traffic characteristics, or unusual land use types) (Basagana et al., 2013). Many prior large LUR studies have been performed at the urban or metropolitan scale, such as a large New York City study which monitored 150 sites across a 777 km^2 area for a sampling density of 0.19 monitors/km^2 (Matte et al., 2013). Our downtown Pittsburgh, PA, USA study is among the most saturated, with 36 distributed sites across 2.8 km^2 (a density of nearly 13 monitors/km^2), drawing out very fine-scale variation in diesel-related organics across a small downtown core.

In this paper, we developed and validated a set of methods for highly-saturated (>10 monitors/km^2) monitoring for very fine-scale spatial gradients in diesel-related pollutants – including both organic and elemental particle constituents, during selected hours of the day. We used land use regression (LUR) methods to examine source-concentration relationships within this microenvironment, and to identify key sources which may explain this variation (Clougherty et al., 2007). We ran geographic information systems (GIS)-based methods to allocate 36 sampling locations across a small (2.8 km^2) domain, using cross-stratification to disentangle impacts of highly-correlated urban vehicular sources (i.e., truck density, bus route intensity, total traffic density). Programmable monitors were configured to collect workweek (Monday–Friday 7 am–7 pm) integrated samples of $PM_{2.5}$, black carbon (BC), elemental constituents, and diesel-related organic compounds [e.g., PAHs, hopanes, steranes], and we used LUR modeling methods to identify key sources explaining spatial variation in each pollutant. We hypothesized that: (1) highly reproducible integrated measures of both elemental and organic components of $PM_{2.5}$ could be captured during selected hours each day, over the course of one week, (2) that concentrations for each pollutant would vary substantially across space, even within this very small area, (3) that spatial patterns and key sources may differ across pollutants – although each was previously associated with diesel, and (4) that LUR models could identify key sources explaining this variation.

2. Materials and methods

2.1. Study domain

Our study domain (roughly 2.8 km^2) is approximately delineated by two major waterway systems which converge and confine the downtown urban core (Fig. 1). The domain boundary includes areas along the opposing riverbanks, and extends to the northwest, to include key source locations of interest (e.g., highways, bridges). The domain was limited to a relatively uniform topography (<274 m above sea level)

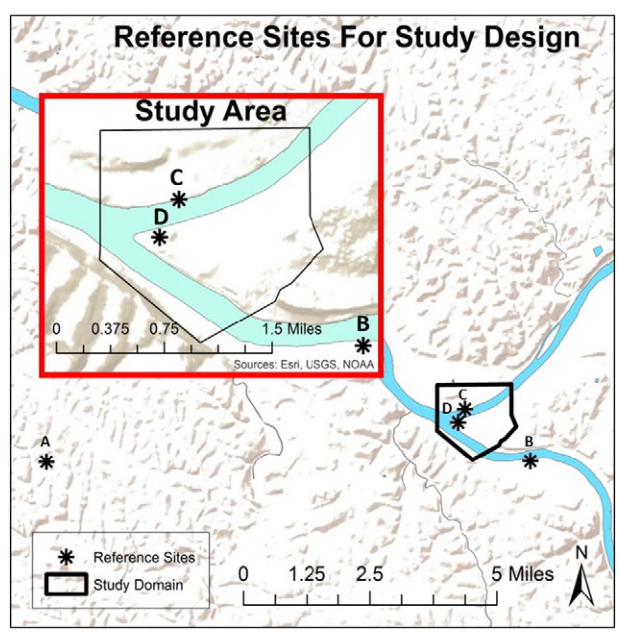

Fig. 1. Four reference monitoring locations in relation to downtown Pittsburgh study domain, with terrain and waterways. Reference A = upwind Settlers Park, Reference B = downwind outside of domain, Reference C = within-domain, Reference D = within-domain Point State Park.

to minimize elevation-related modification of source-concentration relationships.

2.2. Reference monitors

Given our unique study area – situated among complex terrain, bounded by steep hillsides at the confluence of three rivers – meteorological conditions (esp. wind speed and direction) could vary substantially across our study area, altering apparent source-concentration relationships. For this reason, we allocated four reference sites, monitored every session, in very different locations; a regional background site (site A) was situated in a county park, approximately 14.5 km upwind of the study area. Two reference sites were allocated within the study area, on opposing sides of one river (sites C, D). The fourth reference site was sited slightly downwind of the study area (site B), along a second river valley. Weekly average data across these four sites was used to: (1) assess whether long-range transport and/or meteorological impacts on pollutant concentrations have comparable influence across all parts of a complex study area, and (2) to temporally adjust concentrations at all other spatially distributed sites, each sampled only one week per season.

2.3. Site selection and allocation

To characterize our sampling domain in initial explorations, we built and mapped a range of diesel-specific source indicators (e.g., bus routes, total truck traffic, active railways), gasoline traffic indicators (e.g., total traffic density, parking lots), and potential modifying factors (e.g., building height, proximity to rivers). To select sites, we aimed to capture the spatial variability in traffic, and to distinguish diesel from gasoline emissions using highly-resolved GIS-based indicators (e.g., total traffic density, total truck density, bus route frequency). Pennsylvania Department of Transportation (PennDOT) Annualized Average Daily Traffic counts were used to derive a continuous kernel density traffic surface, by applying a Gaussian decay function to traffic counts along roadways. A similar approach was taken for total truck density, using Average Daily Truck Traffic, from the same PennDot dataset. For bus routes, outbound and inbound trips per week were downloaded from Google Transit and summed by route (Google, 2013), then used to derive a kernel density surface. These three surfaces were used to calculate mean source indicator densities using a small 50×50 m lattice grid ($n = 1572$ cells).

For purposes of site allocation – to ensure some variation in source influences across sampling sites – we dichotomized each source indicator at the median, then categorized each 50×50 m grid cell in the domain into binary "high" and "low" source density categories. Using cross-stratification, we created eight source classes (e.g., high traffic/high truck/low truck, etc.); by selecting sites evenly across these categories, we were able to disentangle some effects of these potentially spatially-confounded sources.

We used stratified random sampling (without replacement) to select 36 spatially-distributed grid cells across the eight source indicator cross-strata, and collected one sample within each selected cell, each season. Sample size was determined by resource availability, logistical limitations, and sample size effective in prior LUR modeling studies (Shmool et al., 2014; Brauer et al., 2003; Madsen et al., 2007). In each selected grid cell, we identified street-level metal utility poles close to the cell centroid with (a) no obstructions within three meters, (b) street accessibility, (c) three or more meters from buildings, (d) 20 m from bus stops, and (e) no overhanging tree branches.

To avoid confounding spatial and temporal patterns in concentrations, we randomly allocated distributed sites across sessions, then reviewed schedules by total traffic density strata to ensure reasonably even representation across classes each session (e.g., two to three 'high' and 'low' total traffic density sites per session) (Fig. 2). We sampled five distributed sites per session, and the same sampling schedule was used for both winter and summer ($n = 36$). One site was not sampled due to road closure in the winter, but was sampled during summer.

2.4. Sampled pollutants and instrumentation

Using portable, programmable ambient air sampling units (Matte et al., 2013), we collected integrated samples of $PM_{2.5}$, BC, trace elements, and organic compounds. Briefly, instrumentation included Harvard Impactors (HIs) (Air Diagnostics and Engineering, Inc., Harrison, ME) using 37 mm Teflon™ filters (PTFE membrane, 2 μm pores, Pall Life Sciences) housed in weather-tight Pelican boxes to collect $PM_{2.5}$, BC, and trace elements. We adapted sampling units to collect integrated samples of organic compounds; in separate weather-tight Pelican boxes, organic compounds were collected using cyclone-adapted HIs (Air Diagnostics and Engineering, Inc.) using pre-baked 37 mm quartz fiber filters (Pallflex Tissuquartz non-heat treated filters, Pall Life Sciences). In pilot analyses, gravimetric mass of $PM_{2.5}$ collected on Teflon™ filters using cyclone-adapted HIs was validated against measures collected using standard HIs. HOBO data loggers recorded temperature and relative humidity (Onset Computer Corporation, Bourne, MA). Battery-operated vacuum pumps (SKC, Inc., Eighty-Four, PA) were calibrated to 4.0 LPM and temperature-adjusted based on weather forecasts prior to deployment, and verified after retrieval. Samplers were mounted approximately 3 m above street-level strictly on metal utility poles, to avoid potential contamination by off-gassing volatile organic compounds (VOCs) from treated wooden poles (Gallego et al., 2008).

2.5. Selection of elemental and organic diesel markers

In our prior literature review (Tunno et al., 2015b), 10 elements were previously associated with diesel exhaust in our region; we focus on three that were more commonly associated [aluminum (Al) (Ogulei et al., 2006; Lough & Schauer, 2007), calcium (Ca) (Spencer et al., 2006; Qin et al., 2006; Schauer et al., 2006), and iron (Fe) (Schauer et al., 2006; Rizzo & Scheff, 2007)]. To select organic markers, given relatively greater instability of these compounds, we considered additional criteria, ensuring that each was: (1) previously identified as a marker of diesel exhaust, (2) quantifiable using thermal desorption gas-chromatography mass-spectrometry (TD-GC–MS) or other GC–MS method (Chow et al., 2007), and (3) had lower volatility and reactivity relative to other components of diesel exhaust (e.g., preferably with four or more aromatic rings and higher molecular weight) (Nielson, 1984). Our final list included nine PAHs [benz[*a*]anthracene, benzo[*a*]pyrene, benzo[*e*]pyrene, benzo[*ghi*]fluoranthene, benzo[*ghi*]perylene, chrysene, fluoranthene, indeno[123-*cd*]pyrene, and pyrene], hopanes (homohopane, hopane, norhopane, trisnorhopane), and steranes (cholestanes). A few more reactive compounds (i.e. benz[*a*]anthracene, benzo[*ghi*]perylene, and pyrene) were included for source apportionment (Nielson, 1984; Galarneau, 2008).

2.6. Field protocols for quartz filters

Due to the greater volatility and reactivity of some organic markers, increasing the risks of contamination and sample loss, extra precautions were taken during filter handling in the lab and field. We used pure quartz filters with no binder or glass fibers to reduce reactions with acidic gases, which may produce false readings at low particle concentrations (Pall Life Sciences, 2015). Prior to deployment, quartz fiber filters were placed into porcelain dishes using Teflon-coated tweezers and baked for 4 h at 900 °C (Thermo Scientific Thermolyne oven, Waltham, MA) to remove trace organics, and all cyclone accessories were cleaned using methanol. Inlets were covered with methanol-cleaned aluminum foil to avoid passive contamination. During retrieval, the quartz filter was quickly removed from the cyclone, enclosed in a petri dish, placed inside an insulated box with ice packs, and covered in foil to prevent light exposure. Quartz filters were stored in foil-wrapped

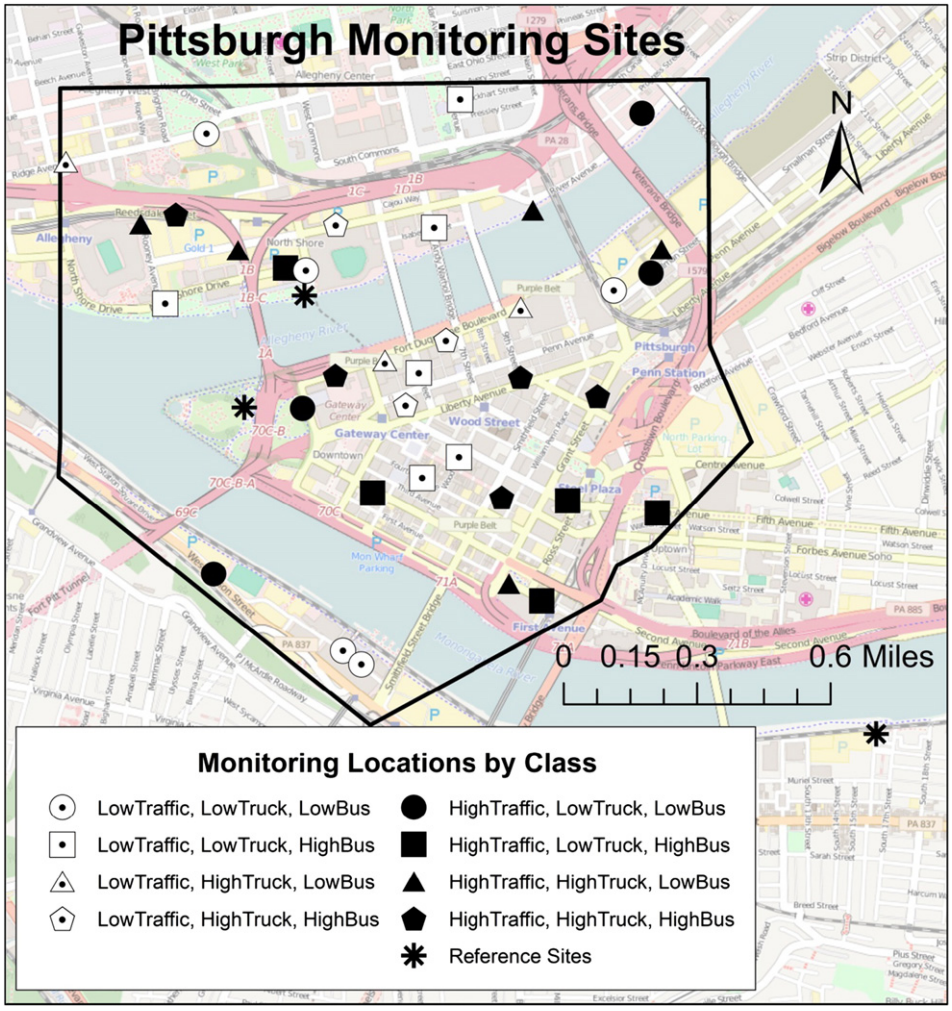

Fig. 2. Downtown Pittsburgh monitoring locations (n = 36) and reference sites by high/low class dichotomization (total traffic density, truck traffic density, bus route density). The upwind reference site outside of the domain (reference site A) is not shown.

petri dishes at −20 °C, until shipped overnight on ice for analysis. Pilot testing established that passive time inside the sampler (i.e., overnight hours) did not interfere with accurate monitoring and characterization of organic compounds.

2.7. Sampling intervals

Samplers were programmed using a chrontroller (ChronTrol Corporation, San Diego, CA), and ran continuously each weekday (Monday through Friday), 7 am to 7 pm, simultaneously across all monitoring locations. The same filter was kept in each sampler throughout the week – such that each filter captures 12 h/day, over five days (60 total hours). Winter sampling was performed from January 14th to March 3rd, and summer sampling from June 10th to August 2nd, 2013. An additional eighth session was performed in the summer, to correct for equipment failure and sample loss at three sites. Deployment and retrieval routes were optimized to minimize travel time and differences in passive time for quartz filters inside samplers at each site, before the 7 am start time.

2.8. Laboratory analyses

Teflon™ filters were pre- and post-weighed within a temperature- and relative-humidity controlled glove box (PlasLabs Model 890 THC, Lansing, MI) using an ultramicrobalance (Mettler Toledo Model XP2U, Columbus, OH) to determine total $PM_{2.5}$ mass. Reflectometry for BC was performed using an EEL43M Smokestain Reflectometer (Diffusion Systems, Ltd., London, UK) and reported in absorbance units (abs). Inductively-coupled plasma mass spectrometry (ICP-MS) was conducted by the Wisconsin State Laboratory of Hygiene following documented protocols (ESS INO Method 400.4; EPA Method 1638) (Sutton & Caruso, 1999). For organic carbon and elemental carbon, thermal-optical reflectance was performed at Desert Research Institute (DRI, Reno, NV) (Chow et al., 1993). TD-GC–MS was conducted by DRI for the selected organic compounds (Chow et al., 2007).

2.9. Quality assurance and quality control (QA/QC)

To assess potential contamination, we collected laboratory blanks and multiple field blanks each session. To assess reproducibility, we deployed an additional unit at four randomly-selected sites each season. All $PM_{2.5}$ and organics samples met acceptable pre- and post-collection flow rates within ±5% of 4.0 LPM. Co-located measures were highly correlated for $PM_{2.5}$, BC, EC, OC, total PAHs, and total steranes (rho = 0.97 to 0.99), and total hopanes (rho = 0.81). Field blanks for multiple pollutants were used to blank-correct all concentrations.

To assess whether concentrations and spatial variation captured during the Monday–Friday 7 am – 7 pm period differed substantially

Table 1
GIS-based source density indicators used for LUR modeling.

Source category for LUR modeling	Covariates examined (25 m to 200 m buffers)	Dataset (year of data)
Traffic density indicators	Mean density of annualized average traffic	Pennsylvania Spatial Data Access (PASDA) (2014)
	Mean density traffic (primary and secondary roads)	Southwestern Pennsylvania Commission (SPC) (2011)
	Number of signaled intersections	
	Annualized average traffic/Aspect ratio	
Road-specific measures	Mean beta index of road complexity and connectivity	TeleAtlas StreetMap (2014)
	Distance to nearest intersection	
	Number of intersections	
	Distance to nearest major road	
	Summed length of primary roadways	PASDA (2014)
	Summed length of primary and secondary roadways	
	Width of roadways	
Truck, bus, and diesel	Mean density of bus traffic	Google Transit Feed (7/14)
	Distance to nearest bus route	
	Distance to nearest bus stop	
	Bus stop use (total number of trips)	
	Mean density of heavy truck traffic on nearest primary roadway	PASDA (2014)
Industrial emissions	Mean density of SO_2 emissions	National Emissions Inventory (NEI) (2011)
	Mean density of $PM_{2.5}$ emissions	
	Mean density of NOx emissions	
	Mean density of VOC emissions	
Land use/built environment	Total area of commercial parcels	Allegheny County Office of Property Assessments (AC OPA) (2013)
	Total area of industrial parcels	
	Total area of industrial and commercial parcels	
	Distance to nearest park	SPC (2011)
	Summed area of parks	
	Building counts	Allegheny County Department of Public Works (DPW)
	Distance to nearest building	National Land Cover Database (NLCD) (2011)
	Mean percentage of imperviousness	
Transportation facilities	Distance to nearest active railroad	SPC (2011)
	Summed line length of active railroads	
	Distance to nearest bus depot	Google Transit (2014)
	Summed area of parking lots and garages	AC OPA (2013)
	Distance to river centerline	PASDA (National Hydrography Dataset, 2014)
Potential modifying factors		
Structural modifiers	Aspect ratio: building height/roadway width	
	Mean building heights	DPW
Topography	Average elevation	National Elevation Dataset (NED) (2013)
	Average slope	NLCD (2011)
	Mean percentage of tree canopy	
Meteorology	Temperature	Obtained from sampler
	Relative humidity	
	Frequency of inversions	Univ. of Wyoming, Dept. of Atm. Science (2013)
	Wind direction	National Oceanic and Atmospheric Association (NOAA) (2013)
	Wind speed	

from results under a 7-day (weeklong) sampling paradigm, we co-located samplers running for five days (Monday–Friday) or seven days (full-week) at eight randomly-selected locations each season. Sampling results were highly correlated ($r = 0.96$–0.99), and comparable spatial patterns were observed under each paradigm.

2.10. GIS-based source density indicators

GIS-based covariates were created for a wide range of sources (Table 1). All covariates were built in terms of distance to a given source (m), or as total source density within relatively small concentric radial buffers around each monitoring location (radius of 25 to 200 m), given our small sampling area and overlap across buffers (reducing variability across sampling sites) at larger buffer sizes. Roadway shapefiles for Pittsburgh (Allegheny County) were obtained from PennDOT's publicly-available annualized average daily vehicle-count data for primary roadways. Traffic covariates included: signaled intersections (number of traffic signals within a given buffer size), mean bus traffic density, mean truck traffic density, and kernel-weighted total traffic density. Bus lines running throughout downtown Pittsburgh were characterized using Google Transit data, number of buses per day on each route derived from Port Authority bus schedules, and bus density throughout the areas calculated by inverse-distance-weighting the bus traffic density on each line using a kernel density tool. Industrial emissions indicators for $PM_{2.5}$ (filterable plus condensable), nitrogen oxides (NO_x), sulfur dioxide (SO_2), and volatile organic chemicals (VOCs) were aggregated from the US EPA's 2011 National Emissions Inventory (NEI) over a six-county region, and interpolated across our study domain using inverse distance weighting (EPA, 2011). Land use zones (i.e., commercial, industrial) were calculated using 2012 assessment data from the Allegheny County Office of Property Assessments. Using the zonal statistics function in GIS, impervious surface, tree canopy, parking garages/lots, parks, building densities and heights, and elevation were also quantified.

2.11. Temporal adjustment

To understand variation in pollutant concentrations across sampling weeks, we compared trends in concentrations of each pollutant across the four reference sites, establishing a common temporal pattern (Fig. 3).

To compare concentrations monitored during different weeks across distributed sampling sites, adjusting for time-varying meteorology or long-range transport, we estimated the expected mean at each distributed site for the entire sampling season. To do so, the observed

concentration at each distributed site was divided by the session-specific mean concentration across the four reference sites, then multiplied by the overall sampling-season mean from the four reference sites, as detailed in (Shmool et al., 2014).

Land-use regression models were constructed for the raw pollutant concentrations, using the weekly mean concentration from the four reference sites as a predictor, and sensitivity-tested using the same suite of source covariates to predict temporally-adjusted concentrations (producing a spatial R^2).

2.12. Statistical analysis

We calculated descriptive statistics for temporally-adjusted $PM_{2.5}$ and BC, total EC and OC, trace elements, and organic compound concentrations, and examined concentration distributions across the source indicator strata used for site selection, using Spearman correlations. We assessed site-specific between-season differences using paired *t*-tests. Potential statistical outliers (outside of mean ± 3 SD) were identified and examined. Data analysis and model-building was performed separately for $PM_{2.5}$, BC, total EC, total OC, groups of diesel-related organics [total PAHs, total hopanes, total steranes], and elements [Al, Ca, and Fe], for summer and winter seasons.

Prior to LUR model-building, the bivariate Spearman correlation between each source indicator and each temporally-adjusted pollutant concentration was examined. The highest correlations between each pollutant and source category were compiled and further considered in modeling. These final candidate covariates for pollutant and season-specific LUR modeling can be found in Supporting information Table S1.

Seasonal LUR models were derived using manual forward step-wise linear regression, to predict raw pollutant concentrations, as described in (Tunno et al., 2015a). Briefly, we first adjusted for background/temporal variation in concentrations, using the mean of the four reference sites for the sampling session. Candidate covariates (source terms) with the strongest bivariate correlation with the temporally-adjusted pollutant were then incorporated into the regression model, individually, in descending order by strength of the bivariate correlation. Only statistically significant covariates ($p < 0.05$) were retained, and the model was assessed using the coefficient of determination (R^2). Covariates were removed, at any stage, if p-values dropped below 0.05, or the variance inflation factor (VIF) became >2.0.

To test for modification in source-concentration relationships by meteorology and structural/topographical characteristics, we tested interaction terms between the retained significant source covariates and median-dichotomized elevation, aspect ratio (building height/roadway width), building height, temperature, wind speed, and wind direction.

Model residuals were mapped to identify systematic spatial variation and locations poorly predicted by the LUR, and to assess any need for additional source covariates. We examined semivariograms and spatial autocorrelation of residuals using the Moran's I statistic.

2.13. Sensitivity analyses

Final covariate selection in each model was sensitivity-tested using scatterplots to assess fit between each significant predictor and raw pollutant concentrations, to ensure that candidate covariates captured variability across the full range of the data, not reliant on outliers or influential points. Tree structures and Random Forest automated methods were used to corroborate covariate selection. All candidate covariates were incorporated into the Random Forest, with over 1000 iterations, and the strongest terms in the output matched the correlations found during LUR model-building. A scatterplot of each retained term against the residual of the prior model was produced at each step in the sequential model-building process, to identify and examine outliers. Model residuals were tested to ensure normality.

To corroborate model fit and covariate selection, we employed backwards elimination for all models, after including all terms with bivariate correlations ≥0.30. For cross-validation of LUR predictions, a random 20% of sites ($n = 7$) were removed from the analysis, and the LUR model was re-fit and used to predict pollutant concentrations at withheld sites. Finally, a boot-strapping approach was applied, and we examined the distribution in R^2.

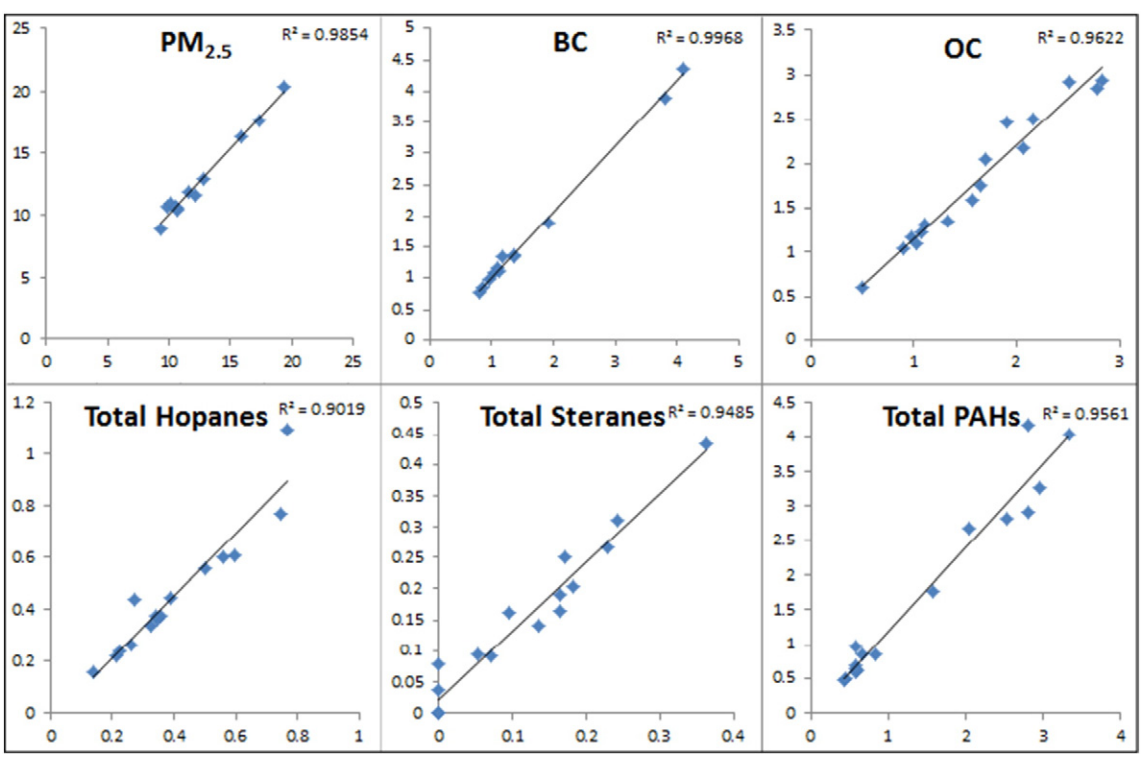

Fig. 3. Co-located monitoring across both seasons indicated high correlations and strong reproducibility of results for multiple pollutants.

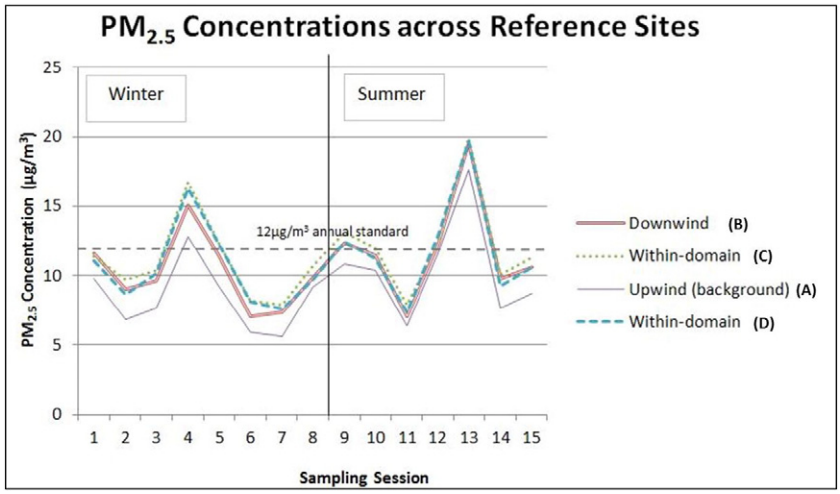

Fig. 4. $PM_{2.5}$ concentrations across reference monitoring sites.

Analyses were performed in SAS v 9.4 (Cary, NC), GIS ArcInfo v 10.1 (ESRI, Redlands, CA), R statistical software v 2.12.1, and Microsoft Excel 2010.

3. Results

We successfully collected all scheduled measurements from the four reference sites, and measures from all 36 distributed sites for the summer season. During winter, one scheduled site could not be sampled due to construction. Only one statistical outlier was identified, for winter season measurements of total PAHs, hopanes, and steranes. Strong correlations were found at co-located monitoring sites (Fig. 3).

3.1. Temporal trends across reference monitors

$PM_{2.5}$ pollutant trends over time were very similar at each of the four reference sites (Fig. 4), and highly correlated across time points (n = 15), indicating a consistent temporal pattern in concentrations across our study area. The upwind monitor (A) correlates strongly with the downtown reference monitors, but is consistently lower in concentration. Likewise, for other pollutants, trends were comparable across the four reference monitors, enabling temporal adjustment as described.

3.2. Summary statistics and spatial patterns

Notably, even across a very small study area, concentrations of $PM_{2.5}$ and most components displayed more variance across sites than

Table 2
Temporally-adjusted pollutant concentrations across 36 distributed sites.

	Winter (n = 35)		Summer (n = 36)		
Pollutant	Mean (SD)	Range	Mean (SD)	Range	p-Value b/w seasons
$PM_{2.5}$ (μg/m^3)	13.22 (2.33)	11.24	13.28 (1.99)	9.45	0.84
BC (abs)	1.49 (0.58)	2.19	1.68 (0.64)	3.06	0.002
Total EC (μg/m^3)	1.30 (0.53)	3.37	1.89 (1.09)	6.42	0.01
Total OC (μg/m^3)	1.89 (0.55)	2.98	2.46 (0.62)	2.30	0.0001
Elemental components (ng/m^3)					
Al	26.69 (20.84)	84.72	35.38 (73.53)	448.71	0.50
Ba	4.29 (2.57)	10.90	4.35 (2.68)	11.71	0.92
Ca	102.90 (95.94)	359.25	96.43 (170.47)	986.12	0.84
Cr	1.04 (0.51)	1.99	1.23 (0.60)	3.22	0.17
Cu	4.82 (2.50)	10.39	5.60 (2.61)	10.50	0.20
Fe	109.10 (55.31)	221.69	127.19 (78.34)	418.74	0.27
Mg	12.07(9.01)	37.62	11.37 (13.00)	58.40	0.79
P	4.15 (2.04)	8.66	4.16 (1.95)	10.63	0.98
S	611.68 (235.31)	1022.57	901.02 (272.08)	1227.21	<0.0001
Zn	17.07 (12.37)	53.27	18.21 (29.07)	178.59	0.83
PAHs (ng/m^3)					
Benz[*a*]anthracene	0.19 (0.07)	0.42	0.27(0.29)	1.25	0.11
Benzo[*a*]pyrene	0.19 (0.12)	0.76	0.20 (0.20)	0.93	0.81
Benzo[*e*]pyrene	0.17 (0.07)	0.41	0.19 (0.09)	0.34	0.21
Benzo[*ghi*]fluor-anthene	0.12 (0.06)	0.36	0.05 (0.07)	0.35	0.001
Benzo[*ghi*]perylene	0.16 (0.21)	1.25	0.10 (0.09)	0.36	0.15
Chrysene	0.33(0.09)	0.55	0.36 (0.20)	1.10	0.40
Fluoranthene	0.29 (0.10)	0.40	0.72 (0.85)	4.49	0.004
Indeno[1,2,3-*cd*]pyrene	0.09 (0.04)	0.22	0.08 (0.04)	0.74	0.55
Pyrene	0.26 (0.11)	0.46	0.51 (0.55)	2.70	0.01
Total PAHs	1.73 (0.65)	3.88	2.45 (1.89)	9.16	0.04
Hopanes and Steranes (ng/m^3)					
Total hopanes	0.43 (0.27)	1.59	0.60 (0.34)	1.65	0.02
Steranes	0.20 (0.19)	1.15	0.03 (0.03)	0.10	0.003

between seasons; temporally-adjusted $PM_{2.5}$ concentrations varied 2-fold across sites in both seasons, although the mean concentrations did not differ by season (Table 2). In both seasons, we observed higher concentrations in the downtown core, and lower concentrations along the rivers (Fig. 5).

Likewise, we found substantial differences across sites for BC, EC, and OC, although mean concentrations were higher in summer than winter ($p < 0.01$). The diesel-related elements (Al, Ca, Fe), total PAHs, and hopanes also varied substantially across sites, but not between seasons. Only total steranes differed more between seasons than across sites, with higher concentrations during winter. For the organic compounds, spatial patterns differed across markers (Table 2, Supplemental Fig. S1).

The 5-day (Monday–Friday 7 am–7 pm period) subset of samples did not spatially differ compared to samples collected over a 7-day (weeklong) sampling paradigm for either season.

3.3. Correlations across modeled constituents

Pollutants were more strongly correlated during winter than summer (See Tables S2 and S3, Supporting information). In winter, we found moderate to high correlations ($p < 0.05$) among several of the modeled pollutants, and lower correlations for those constituents with different spatial patterns.

3.4. LUR model results

Temporal variation, as captured by weekly concentrations at reference monitors, explained substantial variability in $PM_{2.5}$ and wintertime total PAHs, hopanes, and steranes.

In winter, $PM_{2.5}$ was predicted by mean bus density. For summer, measured $PM_{2.5}$ was predicted by mean bus density and area of parking garages (Table 3). A greater proportion of variability in $PM_{2.5}$ was

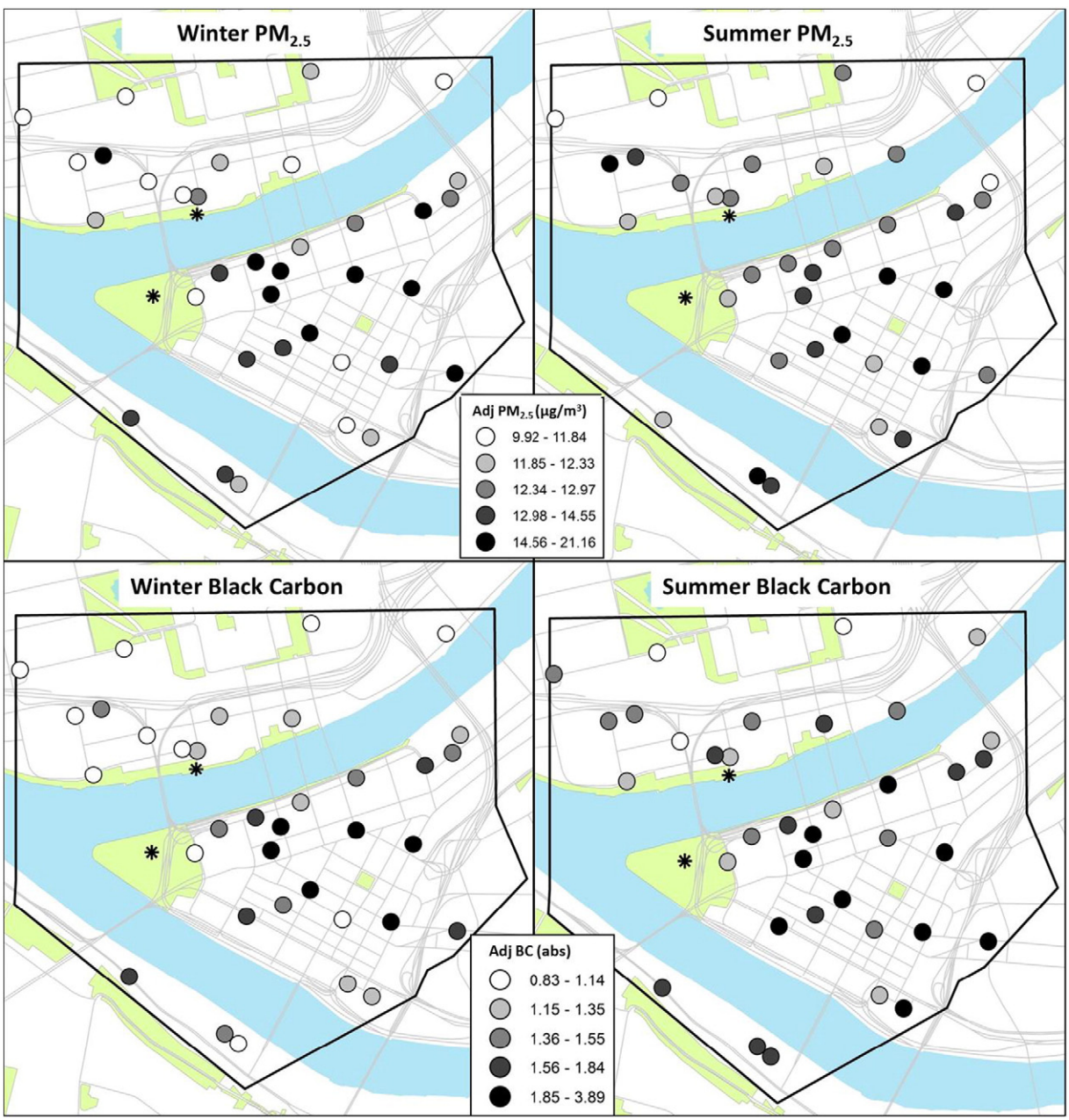

Fig. 5. Temporally-adjusted $PM_{2.5}$ and BC concentrations (in quintiles) across 36 distributed monitoring sites for winter and summer sampling. Asterisks denote the two within-domain reference sites.

explained by meteorology during summer than winter (85% vs. 57%). A greater increase in $PM_{2.5}$ concentrations was attributable to bus density in winter than summer (2.01 vs 0.89 μg/m^3 in $PM_{2.5}$, with a 1-IQR increase in bus density). Between seasons, the best bus density indicator differed in buffer size (i.e. winter = 200 m vs. summer = 50 m).

Winter and summertime LUR models for BC both included bus density terms. Similar proportions of variability (R^2) in BC concentrations were explained by LUR terms in both seasons, with a greater proportion attributable to bus density in winter.

For EC, model terms were identical to those in the BC models for both seasons, although the proportion attributable to temporal variation was much less in the summer than in winter (sequential R^2 = 0.004 vs. 0.23, respectively). For OC, bus stop use was included in both models, although a higher percentage of variability was explained in the winter model.

We identified substantial differences in the models for season-specific concentrations of organic compound groups. Greater temporal contributions were found during winter than summer for all three organics measures (Table 4). In contrast, bus density terms predicted summertime organic concentrations. For total PAHs, the spatial pattern was predicted by mean bus density. For total hopanes, mean bus density and mean truck density explained additional variability. For total steranes, bus stop use predicted additional variability.

We found substantial differences in LUR models for season-specific elemental constituents (Table 5). In the winter, temporal variation explained minimal variation in contributions (R^2 = 0.01 to 0.04), and only bus density explained spatial variability in Al concentrations. In the summer, bus terms were significant for each model. For Al, the spatial pattern was predicted by bus stop use and parking garage area; the Ca model was similar. For Fe, the spatial pattern was explained by mean bus density and parking garage density.

No spatial source terms explained additional variability in the winter organic compounds. Winter concentrations of total hopanes correlated with bus stop use (rho = 0.36) and truck density (rho = 0.43). Winter total steranes correlated with bus stop use within 200 m (rho = 0.52), although none of these terms were retained in final models, after adjustment for temporal variation. This trend held true for winter elemental constituents Ca and Fe, in which only bus density (rho = 0.34) had a modest correlation to Ca.

3.5. Sensitivity analyses

All models were robust to the removal of outliers and influential points. Tree structures and Random Forest automated methods corroborated final covariate selection. *Moran's I* analyses indicated no spatial autocorrelation in model residuals. Removing a randomly-selected subset (20%) of monitoring sites did not significantly change any of the eight models; predicted concentrations at the validation sites were within 10% of measured concentrations.

4. Discussion

Greater variation in concentrations of $PM_{2.5}$ and most constituents was observed across sites than between seasons – even within this small sampling domain. Although the range of concentrations and spatial patterning differed by pollutant, LUR models generally predicted higher concentrations in areas of greater diesel activity, particularly bus route intensity and bus stop use. Though general traffic, truck traffic, and bus traffic each correlated with the majority of our pollutants, the bus effect on pollutant models was substantial and consistent across multiple pollutants. Buses impacted our study area much more strongly than general traffic and trucks. It is possible that our bus metric was a better-built indicator than others in our dataset (Google Transit vs. PennDot data, with inverse-distance weighting), although multiple pollutants are most elevated within the downtown core, where bus traffic is most predominant, substantiating a strong spatial correlation.

For $PM_{2.5}$ and diesel-related trace elements such as Al, Ca, and Fe, no significant differences in concentrations were observed between the summer and winter seasons, possibly due to consistent bus schedules and commuter traffic patterns throughout the year. The consistent traffic patterning may be a plausible reason why the constituent patterning was similar in both seasons for multiple pollutants, with the differences occurring due to varying wind speeds throughout the river valleys and street canyon effects within the downtown core. Furthermore, the small subset of 5-day vs. 7-day samples showed no differences in spatial patterning, indicating that much of the spatial variation in pollution in this area may occur during workweek hours.

Because Pittsburgh is situated among complex terrain, meteorology plays a substantial role in both temporal and observed spatial variations. During winter, lower mixing heights may have trapped pollutants fairly consistently across our relatively flat downtown core, surrounded by rivers and steep escarpments. This interaction between meteorology and terrain – observed to impact spatial patterns in $PM_{2.5}$ and spatial patterns in composition in our prior citywide studies (Shmool et al., 2014; Tunno et al., 2015a; Nielson, 1984) – may have effectively decreased spatial variance within this small area during winter, and increased the relative influence of the temporal term.

An important (though common) limitation was our lack of meteorological (i.e., windspeed and direction) data at each sampling location, limiting our ability to differentiate spatial variance in source effects (e.g., traffic emissions) from structural aspects related to pollutant dispersion (e.g, street canyons). Using regional meteorological data, we

Table 3
LUR model fits for winter and summer $PM_{2.5}$, BC, EC, and OC.

LUR model	Covariates	β (p-value)	IQR conc. increase[a]	Seq R^2[b]
Winter $PM_{2.5}$ (μg/m^3)	Intercept	2.62 (0.07)	–	–
	Weekly ref. PM	0.88 (<0.0001)	–	0.57
	Mean bus density, 200 m	2.2×10^{-8} (0.0002)	2.01	0.72
Winter BC (abs)	Intercept	−0.06 (0.90)	–	–
	Weekly ref. BC	1.26 (0.03)	–	0.19
	Mean bus density, 200 m	7.0×10^{-9} (<0.0001)	0.64	0.59
Winter EC (μg/m^3)	Intercept	−0.24 (0.50)	–	–
	Weekly ref. EC	1.34 (0.004)	–	0.23
	Mean bus density, 200 m	6.0×10^{-9} (<0.0001)	0.55	0.60
Winter OC (μg/m^3)	Intercept	−0.05 (0.92)	–	–
	Weekly ref. OC	1.18 (0.003)	–	0.23
	Bus stop use, 200 m	6.0×10^{-5} (0.05)	0.24	0.52
	Building density, 75 m	0.069 (0.003)	0.41	0.64
Summer $PM_{2.5}$ (μg/m^3)	Intercept	−0.34 (0.64)	–	–
	Weekly ref. PM	1.06 (<0.0001)	–	0.85
	Mean bus density, 50 m	9.0×10^{-9} (<0.0001)	0.89	0.89
	Summed area of parking garages, 125 m	3.2×10^{-6} (0.0002)	1.17	0.93
Summer BC (abs)	Intercept	0.72 (0.09)	–	–
	Weekly ref. BC	0.60 (0.14)	–	0.15
	Mean bus density, 50 m	4.6×10^{-9} (<0.0001)	0.40	0.58
Summer EC (μg/m^3)	Intercept	0.38 (0.40)	–	–
	Weekly ref. EC	0.81 (0.03)	–	0.004
	Mean bus density, 50 m	6.1×10^{-9} (<0.0001)	0.60	0.64
Summer OC (μg/m^3)	Intercept	0.99 (0.02)	–	–
	Weekly ref. OC	0.65 (0.003)	–	0.18
	Bus stop use, 125 m	2.0×10^{-4} (0.01)	0.28	0.36

[a] IQR concentration increase = β*IQR of source indicator.
[b] Seq R^2 is the sequential model fit for each additional term incorporated into model.

Table 4
LUR model fits for winter and summer total PAHs, total hopanes, and total steranes.

LUR Model	Covariates	β (p-value)	IQR conc. increase	Seq R^2
Winter total PAHs[a] (ng/m^3)	Intercept	0.01 (0.95)	–	–
	Weekly Ref. PAHs	1.21 (<0.0001)	–	0.78
Winter total hopanes[a] (ng/m^3)	Intercept	0.09 (0.11)	–	–
	Weekly Ref. hopanes	1.17 (<0.0001)	–	0.49
Winter total steranes[a] (ng/m^3)	Intercept	0.04 (0.08)	–	–
	Weekly Ref. steranes	1.35 (<0.0001)	–	0.52
Summer total PAHs (ng/m^3)	Intercept	−0.16 (0.64)	–	–
	Weekly Ref. PAHs	1.13 (<0.0001)	–	0.41
	Mean bus density, 100 m	1.2×10^{-8} (<0.0001)	0.89	0.66
Summer total hopanes (ng/m^3)	Intercept	−0.13 (0.28)	–	–
	Weekly Ref. hopanes	1.87 (0.0002)	–	0.34
	Mean bus density, 100 m	2.0×10^{-9} (0.05)	0.15	0.55
	Mean truck density, 175 m	2.5×10^{-5} (0.04)	0.16	0.61
Summer total steranes (ng/m^3)	Intercept	0.008 (0.61)	–	–
	Weekly Ref. steranes	0.88 (0.19)	–	0.01
	Bus stop use, 200 m	1.7×10^{-5} (0.001)	0.06	0.43

[a] One outlier removed from LUR analysis.

did not find that either it or elevation gradients modified apparent source-concentration relationships.

Another limitation of our study, also common to many LURs, is limited temporal resolution in source emissions indicators (e.g., annual emissions in NEI data), which is temporally misaligned with our summer and winter sampling periods.

A clear strength of our campaign was the technological capacity to collect filter-based measures across a large number of sites, using programmable units capturing only workweek (Monday–Friday, 7 am–7 pm) hours, capturing reproducible measures of trace organic and elemental constituents. Finally, we were able to capture contemporaneous measures of BC, EC, and OC from all of our sites; because DPM is predominantly carbon, BC is commonly used as a relatively easy-to-measure surrogate for DPM. BC absorbance and EC (thermal-optical) were highly correlated during both summer (rho = 0.95) and winter (rho = 0.95), validating the use of BC as a marker for capturing spatial variance in EC, in our setting.

The data suggests a strong influence of bus-related emissions in the sampled area, especially in the central part of downtown, where there is most congestion and the highest concentration of the public workforce. Signaled intersections also predicted substantial variability in several pollutants, in keeping with the greater prevalence of traffic lights and vehicle idling in the downtown core. Currently, the Port Authority of Allegheny County – the 16th largest public transit agency in the United States, with a fleet of over 700 buses, including 32 hybrid diesel-electric buses – is in the process of updating its fleet to cleaner technologies. All Port Authority buses will be model year 2007 or later by 2020 (Port Authority of Allegheny County, 2013). Other potential interventions which could be explored include re-routing some buses from the dense core with many street canyons trapping pollutants, to the more open perimeters of the small downtown, where winds could better disperse pollutants along the river valleys (albeit in balancing concerns of bus access and convenience). Other interventions could include relocating bus stops to improve traffic flow, adding sensors to improve the timing of traffic lights according to bus flow, and reducing direct human exposures by minimizing bus idling alongside bus stops.

The current study is the most saturated, to our knowledge, with 36 distributed sites across 2.8 km^2 (a density of nearly 13 monitors/km^2), drawing out very fine-scale variation in diesel-related organics across a small downtown core. In contrast, many prior large LUR studies have been performed at the urban or metropolitan scale; a large New York City study monitored 150 sites across a 777 km^2 area (0.19 monitors/km^2), 23 sites were sampled across 98,500 km^2 in Los Angeles (0.0002 monitors/km^2), and 80 sites were sampled across 2199 km^2

Table 5
LUR model fits for winter and summer diesel-related Al, Ca, and Fe concentrations.

LUR model	Covariates	β (p-value)	IQR conc. increase	Seq R^2
Winter Al (ng/m^3)	Intercept	16.58 (0.001)	–	–
	Weekly Ref. Al	−0.16 (0.60)	–	0.01
	Mean bus density, 50 m	5.0×10^{-8} (0.01)	4.97	0.20
Winter Ca (ng/m^3)	Intercept	80.78 (<0.0001)	–	–
	Weekly Ref. Ca	−0.38 (0.49)	–	0.01
Winter Fe (ng/m^3)	Intercept	63.45 (0.05)	–	–
	Weekly Ref. Fe	0.53 (0.27)	–	0.04
Summer Al (ng/m^3)[a]	Intercept	−14.15 (0.13)	–	–
	Weekly Ref. Al	1.31 (0.01)	–	0.18
	Bus stop use, 100 m	9.3×10^{-3} (0.003)	7.10	0.35
	Summed area of parking garages, 175 m	1.8×10^{-5} (0.004)	9.33	0.50
Summer Ca (ng/m^3)[a]	Intercept	−9.14 (0.57)	–	–
	Weekly Ref. Ca	38.40 (0.01)	–	0.10
	Bus stop use, 100 m	0.026 (0.001)	19.86	0.35
	Summed area of parking garages, 150 m	5.7×10^{-5} (0.01)	26.01	0.49
Summer Fe (ng/m^3)[a]	Intercept	−20.97 (0.31)	–	–
	Weekly Ref. Fe	1.29 (<0.0001)	–	0.48
	Mean bus density, 50 m	1.5×10^{-7} (0.02)	15.69	0.56
	Summed area of parking garages, 175 m	3.4×10^{-5} (0.02)	17.62	0.63

[a] One outlier removed from LUR analysis.

in Vancouver (0.04 sites/km^2) (Matte et al., 2013; Moore et al., 2007; Abernethy et al., 2013). The ESCAPE studies across Europe performed LUR modeling using 20 measurements of PM and particle composition,distributed across each of 20 urban study areas of varying size (Eeftens et al., 2012; Wang et al., 2013; de Hoogh et al., 2013).

In sum, we found substantial spatial variation in $PM_{2.5}$, elemental, and organic components during workweek hours with higher concentrations in most pollutants near the center of the downtown core, with substantial bus traffic. Greater variation was found across sites than between seasons, even across this very small area. Measures of bus traffic and bus stop use explained spatial variation in most pollutants, particularly during summer months and at a smaller buffer size, potentially indicating less dispersion. Better understanding spatial variation, during specific hours of peak exposures (i.e., during workweek or commuting hours), across a wide suite of elemental and organic components, can improve air pollution exposure assessment for urban populations, and more clearly point to effective interventions for reducing population exposures and improving population health.

Conflict of interest

The authors declare no conflict of interest.

Acknowledgments

This work was supported by the Allegheny County Health Department (ACHD) Clean Air Fund. The authors would like to thank Jayme Graham, Jason Maranche, Darrell Stern, and Jim Thompson of ACHD for support throughout the project. The authors would like to thank Rebecca Dalton, Sara Gillooly, Jessica McDonald, and R. Tyler Rubright for field work and data support, and Isaac Johnson for GIS support. The authors thank the Pittsburgh Department of Public Works (Alan Asbury and Mike Salem), Duquesne Light Company, and the Allegheny County Department of Parks for monitoring permissions.

Appendix A. Supplementary data

Additional tables regarding source covariates and a figure on organic compound spatial variability can be found in supporting information. Supplementary data associated with this article can be found in the online version, at http://dx.doi.org/10.1016/j.scitotenv.2016.08.011.

References

Abernethy, R.C., Allen, R.W., McKendry, I.G., Brauer, M., 2013. A land use regression model for ultrafine particles in Vancouver, Canada. Environ. Sci. Technol. 47 (10), 5217–5225.

Basagana, X., Aguilera, I., Rivera, M., Agis, D., Foraster, M., Marrugat, J., Elosua, R., Kunzli, N., 2013. Measurement error in epidemiologic studies of air pollution based on land-use regression models. Am. J. Epidemiol. 178 (8), 1342–1346.

Brauer, M., Hoek, G., van Vliet, P., Meliefste, K., Fischer, P., Gehring, U., Heinrich, J., Cyrys, J., Bellander, T., Lewne, M., Brunekreef, B., 2003. Estimating long-term average particulate air pollution concentrations: application of traffic indicators and geographic information systems. Epidemiology 14 (2), 228–239.

Briggs, D.J., de Hoogh, C., Gulliver, J., Wills, J., Elliott, P., Kingham, S., Smallbone, K., 2000. A regression-based method for mapping traffic-related air pollution: application and testing in four contrasting urban environments. Sci. Total Environ. 253 (1–3), 151–167.

CDC, 2003. Monitoring of Diesel Particulate Exhaust in the Workplace.

Chow, J.C., Watson, J.G., Pritchett, L.C., Pierson, W.R., Frazier, C.A., Purcell, R.G., 1993. The DRI thermal/optical reflectance carbon analysis system: description, evaluation and applications in U.S. air quality studies. Atmos. Environ. 27A (8), 1185–1201.

Chow, J.C., Yu, J.Z., Watson, J.G., Ho, S.S., Bohannan, T.L., Hays, M.D., Fung, K.K., 2007. The application of thermal methods for determining chemical composition of carbonaceous aerosols: a review. J. Environ. Sci. Health Part A Tox. Hazard. Subst. Environ. Eng. 42 (11), 1521–1541.

Clougherty, J.E., Levy, J.I., Kubzansky, L.D., Ryan, P.B., Suglia, S.F., Canner, M.J., Wright, R.J., 2007. Synergistic effects of traffic-related air pollution and exposure to violence on urban asthma etiology. Environ. Health Perspect. 115 (8), 1140–1146.

Clougherty, J.E., Wright, R.J., Baxter, L.K., Levy, J.I., 2008. Land use regression modeling of intra-urban residential variability in multiple traffic-related air pollutants. Environ. Health 7, 17.

Cyrys, J., Heinrich, J., Hoek, G., Meliefste, K., Lewne, M., Gehring, U., Bellander, T., Fischer, P., van Vliet, P., Brauer, M., Wichmann, H.E., Brunekreef, B., 2003. Comparison between different traffic-related particle indicators: elemental carbon (EC), PM2.5 mass, and absorbance. J. Expo. Anal. Environ. Epidemiol. 13 (2), 134–143.

de Hoogh, K., Wang, M., Adam, M., Badaloni, C., Beelen, R., Birk, M., Cesaroni, G., Cirach, M., Declercq, C., Dedele, A., Dons, E., de Nazelle, A., Eeftens, M., Eriksen, K., Eriksson, C., Fischer, P., Grazuleviciene, R., Gryparis, A., Hoffmann, B., Jerrett, M., Katsouyanni, K., Iakovides, M., Lanki, T., Lindley, S., Madsen, C., Molter, A., Mosler, G., Nador, G., Nieuwenhuijsen, M., Pershagen, G., Peters, A., Phuleria, H., Probst-Hensch, N., Raaschou-Nielsen, O., Quass, U., Ranzi, A., Stephanou, E., Sugiri, D., Schwarze, P., Tsai, M.Y., Yli-Tuomi, T., Varro, M.J., Vienneau, D., Weinmayr, G., Brunekreef, B., Hoek, G., 2013. Development of land use regression models for particle composition in twenty study areas in Europe. Environ. Sci. Technol. 47 (11), 5778–5786.

Eastwood, P., 2008. Particulate Emissions from Motor Vehicles. John Wiley & Sons, Chichester, England.

Eeftens, M., Beelen, R., de Hoogh, K., Bellander, T., Cesaroni, G., Cirach, M., Declercq, C., Dedele, A., Dons, E., de Nazelle, A., Dimakopoulou, K., Eriksen, K., Falq, G., Fischer, P., Galassi, C., Grazuleviciene, R., Heinrich, J., Hoffmann, B., Jerrett, M., Keidel, D., Korek, M., Lanki, T., Lindley, S., Madsen, C., Molter, A., Nador, G., Nieuwenhuijsen, M., Nonnemacher, M., Pedeli, X., Raaschou-Nielsen, O., Patelarou, E., Quass, U., Ranzi, A., Schindler, C., Stempfelet, M., Stephanou, E., Sugiri, D., Tsai, M.Y., Yli-Tuomi, T., Varro, M.J., Vienneau, D., Klot, S., Wolf, K., Brunekreef, B., Hoek, G., 2012. Development of Land Use Regression models for PM(2.5), PM(2.5) absorbance, PM(10) and PM(coarse) in 20 European study areas; results of the ESCAPE project. Environ. Sci. Technol. 46 (20), 11195–11205.

EPA, 2011. National Emissions Inventory Data. http://www.epa.gov/ttnchie1/net/2008inventory.html (August 10).

Galarneau, E., 2008. Source specificty and atmospheric processing of airborne PAHs: implications for source apportionment. Atmos. Environ. 42, 8139–8149.

Gallego, E., Roca, F.J., Perales, J.F., Guardino, X., Berenguer, M.J., 2008. VOCs and PAHs emissions from creosote-treated wood in a field storage area. Sci. Total Environ. 402 (1), 130–138.

Google, 2013. Google General Transit Feed Specification Project (December).

Hesterberg, T.W., Long, C.M., Bunn, W.B., Lapin, C.A., McClellan, R.O., Valberg, P.A., 2012. Health effects research and regulation of diesel exhaust: an historical overview focused on lung cancer risk. Inhal. Toxicol. 24 (Suppl. 1), 1–45.

Jedynska, A., Hoek, G., Wang, M., Eeftens, M., Cyrys, J., Keuken, M., Ampe, C., Beelen, R., Cesaroni, G., Forastiere, F., Cirach, M., de Hoogh, K., De Nazelle, A., Nystad, W., Declercq, C., Eriksen, K.T., Dimakopoulou, K., Lanki, T., Meliefste, K., Nieuwenhuijsen, M.J., Yli-Tuomi, T., Raaschou-Nielsen, O., Brunekreef, B., Kooter, I.M., 2014. Development of land use regression models for elemental, organic carbon, PAH, and hopanes/steranes in 10 ESCAPE/TRANSPHORM European study areas. Environ. Sci. Technol. 48 (24), 14435–14444.

Kagawa, J., 2002. Health effects of diesel exhaust emissions—a mixture of air pollutants of worldwide concern. Toxicology 181–182, 349–353.

Keuken, M., S., J., Zandveld, P., Voogt, M., 2012. Elemental carbon as an indicator for evaluating the impact of traffic measures on air quality and health. Atmos. Environ. 61, 1–8.

Larson, T., Su, J., Baribeau, A.M., Buzzelli, M., Setton, E., Brauer, M., 2007. A spatial model of urban winter woodsmoke concentrations. Environ. Sci. Technol. 41 (7), 2429–2436.

Lough, G.C., Schauer, J.J., 2007. Sensitivity of source apportionment of urban particulate matter to uncertainty in motor vehicle emissions profiles. J. Air Waste Manage. Assoc. 57 (10), 1200–1213.

Madsen, C., K., L.C., Hoek, G., Oftedal, B., Nafstad, P., Meliefste, K., Jacobsen, R., Nysad, W., Carlsen, K., Brunekreef, B., 2007. Modeling the intra-urban variability of outdoor traffic pollution in slo, Norway - a GA2LEN project. Atmos. Environ. 41, 7500–7511.

Matte, T.D., Ross, Z., Kheirbek, I., Eisl, H., Johnson, S., Gorczynski, J.E., Kass, D., Markowitz, S., Pezeshki, G., Clougherty, J.E., 2013. Monitoring intraurban spatial patterns of multiple combustion air pollutants in New York City: design and implementation. J. Expo. Sci. Environ. Epidemiol. 23 (3), 223–231.

Moore, D.K., Jerrett, M., Mack, W.J., Kunzli, N., 2007. A land use regression model for predicting ambient fine particulate matter across Los Angeles, CA. J. Environ. Monit. 9 (3), 246–252.

Nielson, T., 1984. Reactivity of polycyclic aromatic hydrocarbons toward nitrating species. Environ. Sci. Technol. 18, 157–163.

Noll, J.D., Bugarski, A.D., Patts, L.D., Mischler, S.E., McWilliams, L., 2007. Relationship between elemental carbon, total carbon, and diesel particulate matter in several underground metal/non-metal mines. Environ. Sci. Technol. 41 (3), 710–716.

Noth, E.M., S., H., GS, B., IB, T., 2011. A spatial-temporal regression model to predict daily outdoor residential PAH concentrations in an epidemiologic study in Fresno, CA. Atmos. Environ. 45, 2394–2403.

Ogulei, D., Hopke, P.K., Zhou, L., Patrick Pancras, J., Nair, N., Ondov, J.M., 2006. Source apportionment of Baltimore aerosol from combined size distribution and chemical composition data. Atmos. Environ. 40, 396–410.

Pall Life Sciences, 2015. Pallflex® Filters Product Data. http://www.pall.com/pdfs/Laboratory/02.0601_Pallflex_LR.pdf.

Port Authority of Allegheny County, 2013. Port Authority of Allegheny County provides public transportation throughout Pittsburgh and Allegheny County. http://www.portauthority.org/paac/CompanyInfoProjects/AgencyProfile.aspx.

Qin, Y., Kim, E., Hopke, P.K., 2006. The concentrations and sources of $PM_{2.5}$ in metropolitan New York City. Atmos. Environ. 40, 312–332.

Ristovski, Z.D., Miljevic, B., Surawski, N.C., Morawska, L., Fong, K.M., Goh, F., Yang, I.A., 2012. Respiratory health effects of diesel particulate matter. Respirology 17 (2), 201–212.

Rizzo, M.J., Scheff, P.A., 2007. Fine particulate source apportionment using data from the USEPA speciation trends network in Chicago, Illinois: comparison of two source apportionment models. Atmos. Environ. 41 (29), 6276–6288.

Ross, Z., English, P.B., Scalf, R., Gunier, R., Smorodinsky, S., Wall, S., Jerrett, M., 2006. Nitrogen dioxide prediction in Southern California using land use regression modeling: potential for environmental health analyses. J. Expo. Sci. Environ. Epidemiol. 16 (2), 106–114.

Schauer, J.J., Lough, G.C., Shafer, M.M., Christensen, W.F., Arndt, M.F., DeMinter, J.T., Park, J.S., 2006. Characterization of metals emitted from motor vehicles. Res. Rep. Health Eff. Inst. 133, 1–76 (discussion 77-88).

Schulte, J.K., Fox, J.R., Oron, A.P., Larson, T.V., Simpson, C.D., Paulsen, M., Beaudet, N., Kaufman, J.D., Magzamen, S., 2015. Neighborhood-scale spatial models of diesel exhaust concentration profile using 1-Nitropyrene and other nitroarenes. Environ. Sci. Technol. 49 (22), 13422–13430.

Shmool, J.L., Michanowicz, D.R., Cambal, L., Tunno, B., Howell, J., Gillooly, S., Roper, C., Tripathy, S., Chubb, L.G., Eisl, H.M., Gorczynski, J.E., Holguin, F.E., Shields, K.N., Clougherty, J.E., 2014. Saturation sampling for spatial variation in multiple air pollutants across an inversion-prone metropolitan area of complex terrain. Environ. Health 13 (1), 28.

Spencer, M.T., Shields, L.G., Sodeman, D.A., Toner, S.M., Prather, K.A., 2006. Comparison of oil and fuel particle chemical signatures with particle emissions from heavy and light duty vehicles. Atmos. Environ. 40 (27), 5224–5235.

Sutton, K.L., Caruso, J.A., 1999. Liquid chromatography-inductively coupled plasma mass spectrometry. J. Chromatogr. A 856 (1–2), 243–258.

Sydbom, A., Blomberg, A., Parnia, S., Stenfors, N., Sandstrom, T., Dahlen, S.E., 2001. Health effects of diesel exhaust emissions. Eur. Resp. J. 17 (4), 733–746.

Tunno, B.J., Michanowicz, D., Shmool, J.L.C., Kinnee, E., Cambal, L., Tripathy, S., Gillooly, S., Chubb, L.G., Roper, C., Clougherty, J.E., 2015a. Spatial Variation in Inversion-Focused vs. 24-hour Integrated Samples of PM2.5 and Black Carbon across Pittsburgh, PA. J. Expo. Sci. Environ. Epidemiol.

Tunno, B.J., Dalton, R., Michanowicz, D.R., Shmool, J.L., Kinnee, E., Tripathy, S., Cambal, L., Clougherty, J.E., 2015b. Spatial patterning in PM2.5 constituents under an inversion-focused sampling design across an urban area of complex terrain. J. Expo. Sci. Environ. Epidemiol.

Wang, M., Beelen, R., Basagana, X., Becker, T., Cesaroni, G., de Hoogh, K., Dedele, A., Declercq, C., Dimakopoulou, K., Eeftens, M., Forastiere, F., Galassi, C., Grazuleviciene, R., Hoffmann, B., Heinrich, J., Iakovides, M., Kunzli, N., Korek, M., Lindley, S., Molter, A., Mosler, G., Madsen, C., Nieuwenhuijsen, M., Phuleria, H., Pedeli, X., Raaschou-Nielsen, O., Ranzi, A., Stephanou, E., Sugiri, D., Stempfelet, M., Tsai, M.Y., Lanki, T., Udvardy, O., Varro, M.J., Wolf, K., Weinmayr, G., Yli-Tuomi, T., Hoek, G., Brunekreef, B., 2013. Evaluation of land use regression models for NO2 and particulate matter in 20 European study areas: the ESCAPE project. Environ. Sci. Technol. 47 (9), 4357–4364.